

Pharmacodynamics (PD) and pharmacokinetics (PK) of E7389 (eribulin, halichondrin B analog) during a phase I trial in patients with advanced solid tumors: a California Cancer Consortium trial

Robert J. Morgan¹ · Timothy W. Synold² · Jeffrey A. Longmate³ · David I. Quinn⁴ · David Gandara⁵ · Heinz-Josef Lenz⁴ · Christopher Ruel³ · Bixin Xi² · Michael D. Lewis^{6,8} · A. Dimitrios Colevas^{7,9} · James Doroshow^{1,10} · Edward M. Newman²

Received: 27 July 2015 / Accepted: 2 September 2015 / Published online: 11 September 2015
© Springer-Verlag Berlin Heidelberg 2015

Abstract

Background The California Cancer Consortium completed a phase I trial of E7389 (eribulin mesylate), an analog of the marine natural product halichondrin B. This trial was to determine the pharmacodynamics, pharmacokinetics, and MTD of E7389 administered by bolus injection weekly for 3 weeks out of four.

Methods This trial included a rapid titration design. Real-time pharmacokinetics were utilized to guide dose escalation. Initially, single-patient cohorts were enrolled with intra- and inter-patient dose doubling. The second phase was a standard 3 + 3 dose escalation schedule. At the MTD, a cohort of patients was enrolled for target validation studies (separate manuscript). The starting dose was 0.125 mg/m², and doses were doubled within and between patients in the first phase. Blood and urine sampling for

E7389 pharmacokinetics was performed on doses 1 and 3 of cycle 1. Levels were determined using a LC/MS/MS assay.

Results Forty patients were entered. Thirty-eight were evaluable for toxicity and 35 for response. The rapid escalation ended with a grade 3 elevation of alkaline phosphatase at 0.5 mg/m²/week. The second phase ended at 2.0 mg/m²/week with dose-limiting toxicities of grades 3 and 4 febrile neutropenia. Other toxicities included hypoglycemia, hypophosphatemia, and fatigue. The MTD was 1.4 mg/m²/week. Responses included four partial responses (lung cancer [2], urothelial [1], and melanoma [1]).

Conclusions E7389 was well tolerated in this trial with the major toxicity being myelosuppression. PD shows that E7389 induces significant morphologic changes (bundle formation) in the microtubules of peripheral blood mononuclear cells and tumor cells in vivo. The data suggest that lower intra-tumoral levels of β -tubulin III or higher intra-tumoral levels of MAP4 may correlate with response to

Reported in part in Proc. Amer. Soc. Clin. Oncol. 22:A575, 2003, and 23:A3036, 2005, and in Proc. Amer. Assoc. Cancer Res. 44:A5344, 2003.

✉ Robert J. Morgan
rmorgan@coh.org

¹ Department of Medical Oncology and Therapeutics Research, City of Hope Comprehensive Cancer Center, 1500 E. Duarte Rd., Duarte, CA 91010, USA

² Department of Cancer Biology, City of Hope Comprehensive Cancer Center, Duarte, CA 91010, USA

³ Department of Biostatistics, City of Hope Comprehensive Cancer Center, Duarte, CA 91010, USA

⁴ Division of Medical Oncology, University of Southern California, Norris Comprehensive Cancer Center, Los Angeles, CA 90033, USA

⁵ Division of Medical Oncology, University of California, Davis Cancer Center, Sacramento, CA, USA

⁶ Eisai Research Institute, Andover, MA 01810, USA

⁷ Division of Cancer Treatment and Diagnosis, National Cancer Institute, Bethesda, MD 20892, USA

⁸ Present Address: Edward P. Evans Foundation, Casanova, VA 20139, USA

⁹ Present Address: Stanford Cancer Center, Stanford, CA 94305, USA

¹⁰ Present Address: Division of Cancer Treatment and Diagnosis, National Cancer Institute, Bethesda, MD 20892, USA

E7389, while lower intra-tumoral levels of stathmin may be associated with progression. PK data reveal that E7389 exhibits a tri-exponential elimination from the plasma of patients receiving a rapid i.v. infusion. At sub-toxic doses, plasma concentrations of E7389 are maintained well above the levels required for activity *in vitro* for >72 h.

Keywords Pharmacodynamics · Pharmacokinetics · Eribulin · Halichondrin B analog · Phase I trial

Introduction

New drug development requires preclinical testing in cell line and animal models, and phase I and II clinical testing to determine toxicity and efficacy [1], and pharmacokinetic and correlative studies to elucidate the mechanisms of activity. The goals are to demonstrate that the agent is reaching the tumor and having the desired effect on its molecular target and to gain preliminary information about differential activity in patient groups.

Agents that target the cell cycle and inhibit cell division [2, 3] include E7389 (eribulin mesylate, NSC 707389), a tubulin inhibitor which is a modified and synthetically produced analog of the marine natural product halichondrin B. This agent inhibits microtubule dynamics by mechanisms that are distinct from all other tubulin-binding agents [4–15].

Preclinical data reveal that sub- to low-nanomolar levels of E7389 inhibit cancer cell proliferation by the induction of a cell cycle block at G2/M, disruption of mitotic spindles, and initiation of apoptosis [4, 16], and tumor xenograft studies in athymic mice demonstrated tumor regression, remission, and increased life span at dosing levels below the maximally tolerated dose (MTD) [4], suggesting that E7389 has a wide therapeutic window relative to other cytotoxic anticancer agents. In-depth studies have confirmed E7389's novel mechanism of action with respect to inhibition of microtubule dynamics [5]. This is a report of the pharmacodynamics and pharmacokinetics of E7389 determined during a phase I study and describes the correlative studies which were performed to demonstrate the *in vivo* antimetabolic activity of E7389 in pre- and post-treatment tumor biopsies and to investigate the relationship between tumor expression of microtubule-associated genes and clinical outcomes.

Patients and methods

Patient selection

Forty patients with advanced, histologically confirmed solid tumors were entered on this trial. Patients were required to have chemotherapeutically unresponsive

malignancies, to have relapsed following previous chemotherapeutic regimens, or to have malignancies for which no “standard” chemotherapeutic regimen exists. Eligibility requirements included a Karnofsky performance status (KPS) of at least 60 %, age ≥ 18 years, and an expected survival of at least 2 months. Adequate renal (24-h creatinine clearance of ≥ 60 mL/min), bone marrow (absolute neutrophil count ≥ 1500 /dL and platelet count $\geq 100,000$ / μ L), and hepatic (serum bilirubin ≤ 1.5 mg/dL, and SGOT and SGPT within 2.5 times the institutional upper limit of normal) were required. Prior chemotherapy must have been completed at least 4 weeks prior to beginning treatment on this protocol [6 weeks for nitrosoureas and 8 weeks for 7-hydroxystaurosporine (UCN-01)], and patients must have recovered from side effects of prior therapy. There was no limit on the number of prior courses or types of chemotherapy. Patients with brain metastases were ineligible for this study. Because the safety of E7389 to the unborn fetus has not been established, pregnant patients and patients who were breast feeding were ineligible. All patients of child-bearing potential, both male and female, were advised to practice adequate contraception. Premenopausal women must have had a negative pregnancy test prior to entry on this study. Due to concerns regarding possible drug interactions, patients with HIV taking antiretroviral medications were ineligible. All patients were required to have evaluable disease. The presence of measurable disease was not required for this phase I study. Patients with any non-malignant intercurrent illness which was poorly controlled were ineligible. Patients may not have received concurrent therapy with any other antineoplastic therapy.

All patients gave their voluntary informed consent and signed a consent document that had been reviewed and approved by the Institutional Review Boards of the City of Hope National Medical Center, the University of Southern California, or the University of California, Davis.

Pre-treatment evaluation

All patients had a complete history and physical examination performed including documentation of weight, Karnofsky performance status (KPS), presence of measurable or evaluable disease, and a complete blood count with platelet count and differential, 18 channel blood chemistry analysis, chest X-ray (if indicated), and computed tomographic scans of the chest, abdomen, and pelvis as needed to document measurable or evaluable disease. Pre-treatment blood analyses must have been performed no earlier than 72 h prior to each cycle of chemotherapy; pre-treatment radiographic examinations must have been completed no earlier than 2 weeks prior to the first cycle of chemotherapy. Patients were required to have repeated radiographic procedures no less often than every 8 weeks.

Treatment plan

Blood samples and tumor biopsies were obtained before the first cycle. E7389 was administered as an intravenous bolus over 1–2 min weekly for 3 weeks. It was supplied as a 500 µg/mL solution in ethanol/water (5:95) in 1 mL vials and was administered intravenously without further dilution. Plasma and urine were obtained for pharmacokinetic studies during cycle one on days 1 and 15. A complete cycle was defined as 4 weeks.

Treatment cycles were repeated after a 1 week. Treatment cycles may have been delayed for up to 14 days to allow for recovery from toxicities. Patients unable to safely resume treatment within 14 days were taken off study. All patients with progressive disease were taken off treatment. Patients with stable disease or objective responses, and without unresolved dose-limiting toxicity (DLT), were able to receive repeat cycles indefinitely at the discretion of the treating physician.

Statistical methods and definition of toxicities

This trial was a phase I study of the California Cancer Consortium and included the City of Hope (COH) Comprehensive Cancer Center, University of Southern California/Norris Comprehensive Cancer Center, and the University of California, Davis Cancer Center. Registration and assignment to the dose level were done centrally at COH.

An accelerated titration design, design 4B described by Simon et al. [17], was used which permitted intra-patient dose escalation for patients who had not experienced any toxicity worse than grade 1 on any dose level. It also utilized an initial accelerated dose escalation stage that ended by the occurrence of a single (DLT) (grade 3 or 4) or two occurrences of moderate toxicity (grade 2). The initial dose escalations were therefore based on all of the accumulated toxicity history for all patients. When the initial accelerated stage of accrual ended, subsequent dose escalations were based on toxicities occurring in each patient during the first cycle of treatment. Toxicity was graded according to the NCI Common Toxicity Criteria, version 2.0. To be evaluable for toxicity, a patient must have experienced a DLT or have received at least one complete cycle of treatment and be followed for at least 28 days. Inevaluable patients were replaced, but all enrolled patients receiving any amount of protocol therapy were evaluated for toxicity and included in the summaries of results.

In order to safely conduct the two-part escalation scheme, it was necessary to define “moderate” toxicity in addition to DLT. Any toxicity or adverse event not present at baseline was eligible to meet the definition of either DLT or “moderate” toxicity regardless of attribution. “Moderate” toxicity was defined as any grade 2 toxicity, except

allergic rhinitis, fatigue, sweating, weight gain or loss, alopecia, dry skin, nail or pigmentation changes, pruritus, hot flashes, flatulence, mouth dryness, nausea and vomiting without the use of maximal anti-emetic treatment, sense of smell or taste disturbance, erectile impotence, irregular menses, loss or gain of libido, oligospermia, or tumor flare or lysis syndrome.

Non-hematologic DLT was defined as any grade 3 or 4 toxicity, except nausea and vomiting without the use of maximal anti-emetic treatment, female sterility or male infertility, or tumor flare or lysis syndrome. Hematologic DLT was defined as any grade 4 thrombocytopenia, grade 4 neutropenia not reversible to \leq grade 3 within 120 h, febrile neutropenia, and neutropenia associated with bacteremia or sepsis (anemia or lymphopenia of any grade was not a DLT.)

The MTD was defined as the highest dose tested in which no more than one of the first six patients evaluable for toxicity experienced DLT in the first cycle and is one dose level below the lowest dose tested in which two or more patients experienced DLT in the first cycle. At least six patients were treated at the MTD.

Starting dose and schedule

The starting dose of E7389 was 0.125 mg/m² administered as an intravenous bolus over 1–2 min weekly for 3 weeks of a 4-week cycle. This dose was chosen based on observed toxicities of E7389 in mice, rats, and dogs [18]. In toxicology studies, the agent produced bone marrow depression in dogs and rats, intestinal toxicity in dogs, and liver toxicity in rats when administered intravenously once daily on days 1, 5, and 9. The starting dose for E7389 was <1/10 of the MTD in rats and <1/3 of the toxic dose in dogs.

Dose escalation

The occurrence of DLT and moderate toxicity for all patients on all courses was recorded and maintained at the data coordinating center. Because of the limited amount of preclinical toxicology data available for E7389 at the time that this trial was performed, and the conservative starting dose, a two-part escalation scheme was used [17]. The planned dose levels increased in one-half log (approximately 40 %) increments so that two dose escalation steps doubled the dose. Initially, cohorts consisted of a single patient, and the dose of E7389 was doubled, i.e., escalated by two dose levels, for each new cohort. During the initial accelerated escalation stage of the trial, patients eligible for continued treatment had their doses escalated by 100 % (two dose levels) if they had not experienced toxicity worse than grade 1. The accelerated escalation stage was stopped when “moderate” toxicity was encountered

in a total of two patients (cumulative across all dose levels and courses) or DLT was encountered in one patient. The cohort at that dose was then expanded to three patients and continued into the second stage of accrual. A minimum of three patients was entered at each dose level during the second stage of the escalation.

If 0/3 patients experienced a DLT, three patients were then treated at the next dose level. If DLT was experienced in exactly one of three patients, three additional patients (for a total of six) were treated at that dose level. If no additional DLTs were observed at the expanded dose level (i.e., 1/6 with DLT), the dose was escalated by one level. Escalation terminated when two patients experienced DLTs at a given dose level, following which the dose was de-escalated one level at a time. If six patients had not yet started at the next lower dose level, that level was expanded to six patients. De-escalation ended when the maximally tolerated dose was established, i.e., when the maximum dose was found where no more than one of six evaluable patients experienced a DLT on the first course. Following the determination of the MTD, additional patients were accrued at that dose level until evaluable post-treatment biopsy material was obtained on ten patients in order to validate the molecular targets of E7389 in man.

All patients on each dose level who had not experienced DLT were observed for a minimum of 2 weeks following the day 15 dose on cycle one before the dose level was escalated.

E7389 pharmacokinetics

Patients were asked to give a total of 16 blood samples [5 mL of blood per sample] and two 24-h urine collections over a 3-day period following doses 1 and 3 of the first cycle. In addition, the pharmacokinetic sample collections were repeated on doses 1 and 3 of subsequent cycles whenever an intra-patient dose escalation occurred during the accelerated phase. Blood samples were kept on ice and processed within 1 h of phlebotomy. Processing consisted of separation of plasma from whole blood by centrifugation at 1500× rpm for 10 min at 4 °C. Plasma was transferred to appropriately labeled polypropylene tubes and stored at <−70 °C until shipping. Following the completion of each urine collection, the total volume of urine was recorded and an aliquot was frozen for drug level analysis. Plasma and urine samples collected for determination of E7389 were kept frozen at <−70 °C until all the samples for each course were collected.

E7389 in plasma and urine was determined using an LC–MS/MS assay method developed and validated in the City of Hope Analytical Pharmacology Core facility. Following addition of an internal standard (ER-076349) and acidification with hydrochloric acid, plasma, and urine

were extracted with six volumes of dichloromethane. The organic phase was evaporated to dryness, reconstituted in mobile phase, and analyzed by gradient LC separation on a C18 column with tandem mass spectrometry detection. Recoveries of E7389 and internal standard from plasma and urine by this method were >60 %. The mass spectrometry settings were as follows: capillary voltage = 2.90 kV, cone voltage = 58 V, collision cell voltage = 18 V, source temperature = 125 °C, desolvation temperature = 300 °C, cone gas flow = 150 L/h, and desolvation gas flow = 550 L/h. The mass transitions monitored for E7389 and internal standard were 730.5 → 712.5 and 731.6 → 681.4 m/z, respectively. Intra- and inter-day precision and accuracy of the method were within ±10 % of target values over the entire range of the standard curve, with a LLOQ of 0.1 ng/mL from a starting sample volume of 0.2 mL.

Pharmacokinetic data analyses were performed using both compartmental and non-compartmental methods. Compartmental analyses were performed using ADAPT II software (USC Biomedical Simulations Resource, Los Angeles, CA, USA), and non-compartmental analyses were performed using the rule of linear trapezoids. Individual pharmacokinetic parameter estimates (e.g., CL_{sys} , V_d , $t_{1/2}$, and AUC) were determined for each patient and tabulated by dose level with summary statistics (medians, means, and standard deviations). Individual parameter estimates obtained for doses 1 and 3 were compared using two-tailed Student's *t* test.

E7389 pharmacodynamics

Following determination of the MTD in the clinical trial, an additional 13 patients with accessible tumors were enrolled at this dose to obtain pre- and post-treatment biopsy material for an exploratory evaluation of molecular correlates to validate the molecular targets of E7389 in man. To maximize the likelihood of obtaining tissue from patients treated in the expanded MTD cohort, only patients with tumors appropriate for repeated biopsy were eligible during this stage of the study. Fresh tumor biopsies for the correlative studies were obtained before treatment and then 1 and 24 h after dose 1 of cycle 1. Fresh tissue was sectioned longitudinally by a pathology technician for histologic evaluation, and the remaining tissue was fixed in formalin, paraffin-embedded (FFPE), and stored for analysis of mRNA levels of genes that may be involved in response to E7389. In addition, in a single patient with NSCLC and a large involved axillary lymph node, sufficient tumor tissue was available to make slides for serial fluorescent immunohistochemical analysis of cytoskeletal morphology.

Serial pre- and post-E7389 treatment FFPE tissue specimens were sent to Response Genetics Inc. (RGI, Los

Table 1 Dose-level summary

Dose level (mg/m ²)	No. of patients	No. of patients w/ Crs 1, grade 3/4 tox.	No. of patients w/ Crs 1, grade 3/4 tox. related	Patients w/ DLT	Total completed courses (no. pts)	Objective responses
0.125	1	0	0	0	2 (1)	
0.18					0	
0.25	1	0	0	0	8 (1)	
0.35					0	
0.5	7	4	2 [lymphopenia (1)]	1 (alkaline phosphatase)	12 (7)	
0.7	4	3	2	0	14 (4)	
1.0	3	1	0	0	5 (3)	
1.4	19	14	10	1 (febrile neutropenia)	80 (19)	PR: lung, bladder, melanoma
2.0	5	4	4	2 (febrile neutropenia)	21 (5)	PR: lung

PR partial response, Crs course

Angeles, CA, USA) for quantitative analysis of expression of β -tubulin isotypes (III, IVb, V, and VI), MAP4, and stathmin. Specimens were reviewed by the RGI pathologist, and tumor was separated from normal tissue by microdissection. RNA was extracted from the microdissected fixed tissue using a RGI-patented technology, and cDNA was synthesized by random-primed reverse transcription. Quantitative PCR was performed using gene-specific primers and probes on an ABI Prism 7900 TaqMan. Data were reported from samples that generated results within the validated range of each gene-specific assay.

For analysis of changes to cytoskeletal morphology following E7389 treatment, slides were cut from serial FFPE tumor blocks from a single patient. Cytospins were made from peripheral blood mononuclear cells (PBMC) collected in parallel with tumor tissue for comparison. Analysis consisted of fluorescent immunohistochemical assessment of α -tubulin and chromatin. Briefly, slides were treated with a primary antibody directed against α -tubulin (Sigma Chemical, St. Louis, MO, USA) for 1 h at room temperature. After thorough washing, slides were incubated with and FITC-labeled secondary antibody (Sigma Chemical, St. Louis, MO, USA) for 1 h at room temperature. After another round of washing, slides were incubated with propidium iodide for chromatin staining. Stained slides were imaged using an Olympus IX81 inverted digital fluorescent microscope fitted with a Spot RT (real time) digital camera, and image analysis was performed using Image Pro software (Media Cybernetics, Inc., Silver Spring, MD, USA). Separate images were acquired for tubulin and chromatin, and the final image was obtained by merging the separate data files.

Results

Patient characteristics

Forty patients enrolled on this phase I trial received 142 (median 2, range 1–14) courses of treatment (Table 1). Patient characteristics are summarized in Table 2. Twenty patients were male and twenty were female. The median age was 61 years (range 27–84), and the median KPS was 80 % (range 60–100 %).

Dose-limiting toxicities of therapy

The dosage escalation and toxicity by dose level are summarized in Table 1. Three patients were treated during the accelerated dose escalation portion of the protocol. The first two patients treated at 0.125 and 0.25 mg/m²/week experienced no grade 3 or 4 toxicities. The first patient treated at 0.5 mg/m²/week experienced a self-limited elevation of alkaline phosphatase which qualified as a DLT. The dose level was then expanded to six evaluable patients. Of these, one patient experienced non-dose-limiting lymphopenia. Four patients were then accrued to the next dose level (0.7 mg/m²/week). One of these was inevaluable due to non-completion of the first course of treatment due to unforeseen schedule changes. Two patients experienced non-dose-limiting grade 3 toxicity including neutropenia and lymphopenia. Three patients were then entered at 1.0 and 1.4 mg/m²/week, none of whom experienced dose-limiting toxicity. The first patient entered at 2 mg/m²/week developed febrile neutropenia, and the dose level was then expanded. The fifth patient on this dose level also experienced grade 4

Table 2 Patient characteristics

Gender	
Female	20
Male	20
Race	
Caucasian	34
Asian	5
African-American	1
Karnofsky performance status (%)	
90–100	15
70–80	24
60	1
Histologic types	
Lung	10
Breast	7
Transitional cell	
Renal pelvis	2
Bladder	2
Ureter	1
Melanoma	2
Ovary	2
Other (see text)	14
Age in years [median (range)]	61 (27–84)
Prior treatment	
Surgery	40
Radiation	21
Chemotherapy	39

dose-limiting neutropenia. The 1.4 mg/m²/week dose level was expanded to six evaluable patients. One of the additional three patients experienced febrile neutropenia, thus establishing the maximally tolerated dose. Other non-dose-limiting episodes of grade 3/4 neutropenia and fatigue were also observed at this dose level. Thirteen additional patients were entered in an expanded cohort in order to obtain additional toxicity information, plasma, and biopsies of tumor. Further episodes of non-dose-limiting neutropenia and fatigue were noted in the expanded cohort as documented in Table 3.

Grade 3 or 4 dose-limiting toxicities are summarized in Table 1, while non-dose-limiting toxicities are listed in Table 3 and included metabolic disturbances of hyperglycemia and hypophosphatemia. Neurologic toxicities included single episodes of non-neuropathic muscle weakness and sensory neuropathy. One episode of severe nausea and vomiting was noted in one patient. Dermatologic toxicity including a radiation recall reaction and an episode of rash/desquamation was noted in subsequent courses.

Courses completed, responses, and reasons for discontinuation of protocol therapy

The number of courses administered per dose level is summarized in Table 1. The median number of courses completed across all dose levels was 2 (range 1–14). Of the 40 patients enrolled, 35 were evaluable for response. Three patients treated with 1.4 mg/m²/week had partial responses. One patient with non-small cell lung cancer on the 2 mg/m²/week dose level achieved a partial response that lasted for multiple cycles. However, treatment was discontinued after course 10 due to grade 3 neuropathy. The patient did not progress until he had been off treatment for several months. One patient with non-small cell lung cancer achieved a partial response following four courses of treatment: the tumor then progressed following an additional two cycles; one patient with bladder cancer received ten courses of treatment and then stopped treatment due to physician choice; and one patient with melanoma achieved a partial response following two courses of treatment. This patient's treatment was discontinued due to excessive neutropenia. Fourteen additional patients who received a median of 6 courses (range 2–14) achieved stable disease prior to tumor progression.

Pharmacokinetics

Due to the low starting doses of E7389 used in this trial, a sensitive assay method was required for the performance of the pharmacokinetic studies. Investigators in the City of Hope Analytical Pharmacology Core Facility developed and validated a LC–MS/MS assay with a lower limit of detection of 0.15 nM E7389. Twenty-nine patients were evaluable for the first-dose pharmacokinetic studies, and two of these patients had intra-patient dose escalations with additional pharmacokinetics. The parameters are summarized in Table 4. The mean E7389 body surface area-adjusted CL_{sys} and V_d were 1.5 ± 0.7 L/h/m² and 67.3 ± 66.6 L/m², respectively. Mean plasma α, β, and γ half-lives were 11.8 ± 6 min, 1.9 ± 1.6, and 50.0 ± 46.2 h, respectively. Figure 1 depicts the plasma concentration versus time profile for E7389 on doses 1 and 3. As shown in the figure, E7389 exhibits a tri-exponential elimination from the plasma of patients receiving a rapid i.v. infusion (over 1–2 min). Following a rapid distributive phase, E7389 is slowly eliminated with a terminal elimination half-life in the range of 36–48 h. Despite the long terminal half-life, no significant accumulation was seen between doses 1 and 3. The systemic clearance of E7389 is unrelated to the dose over the range of doses tested. Figure 2 demonstrates the apparent linear relationship between measured drug

exposures (e.g., AUC) and dose levels. The apparent volume of distribution of E7389 is significantly greater than vascular volume. At sub-toxic doses, plasma concentrations of E7389 are maintained well above the levels required for activity in vitro for >72 h. Renal clearance of E7389

accounted for only a minor percentage ($10 \pm 1 \%$) of the total drug elimination (data not shown).

Tissue sampling for microtubule targeting and gene expression studies

In order to validate the microtubule network as the therapeutic target of E7389, peripheral blood mononuclear cells and tumor tissues were collected for serial analysis of microtubule morphology by fluorescent immunohistochemistry. A single patient with an accessible site of disease (NSCLC) consented to provide serial biopsy specimens prior to and then 1 and 24 h following his first dose of E7389. Cytospins were prepared from peripheral blood mononuclear cells (PBMC) obtained at the times corresponding to the biopsies. Slides were prepared from the formalin-fixed paraffin-embedded tumor tissue, and then, both the tumor slides and cytospins were dual stained for β -tubulin and DNA visualization by fluorescent microscopy. As shown in Fig. 3, E7389 induces significant morphologic changes (bundle formation) in the microtubules of peripheral blood mononuclear cells and tumor cells in vivo. These results are very similar to data obtained from patients receiving another anti-microtubule acting agent, epothilone B analog [19], indicating that the drug is reaching the tumor tissue and acts on its presumed target.

Thirty-six serial biopsies specimens were obtained from 13 patients treated at the MTD. Following pathology review, 11 subjects were determined to have specimens adequate for tumoral gene expression analysis. Tumoral expression of β -tubulin isotypes (class III, IVb, V, VI), MAP4, and stathmin was determined by quantitative PCR. Because gene expression from specimens collected pre-treatment and post-treatment did not vary significantly (data not shown) and because pre-treatment specimens were not available from all subjects, the data were reported as the average gene expression for all samples collected

Table 3 Other non-DLT-related grade 3/4 toxicities across all dose levels

Toxicity (grade 3/4)	Number of episodes
<i>Course 1</i>	
Hematologic	
Total white count	7
Neutrophils/granulocytes (3/4)	14
Febrile neutropenia (expanded cohort)	2
Port infection	1
Lymphopenia	1
Metabolic	
Hyperglycemia (3)	1
Hypophosphatemia (3)	1
Alkaline phosphatase (3)	1
Neurologic	
Muscle weakness—not neuropathy (3)	1
Fatigue (4)	1
Nausea/vomiting (3)	1
<i>All other courses</i>	
Dermatologic	
Radiation recall reaction (course 3) (4)	1
Rash/desquamatization (course 2) (3)	1
Hematologic	
Total white count (3)	5
Neutrophils/granulocytes (3/4)	25
Lymphopenia (3)	1
Metabolic	
Hyperglycemia (3)	2

Table 4 Summary of dose 1 E7389 pharmacokinetic parameters

Dose level (mg/m ²)	<i>N</i>	CL _{sys} (L/h)	CL/m ² (L/h/m ²)	<i>V</i> _d (L)	<i>V</i> _d /m ² (L/m ²)	<i>T</i> _{1/2} α (min)	<i>T</i> _{1/2} β (h)	<i>T</i> _{1/2} γ (h)	AUC (nM h)
0.1	1	2.6	1.3	68.9	35.5	23.6	2.8	34.3	127.5
0.3	2	2.0	1.0	87.9	43.4	25.4	3.4	47.6	355.3
0.5	8	2.7	1.4	110.8	57.2	11.1	2.5	42.3	576.5
0.7	4	2.0	1.1	88.7	49.5	15.3	1.7	43.9	967.5
1.0	3	1.9	1.1	72.6	40.8	13.7	1.7	43.4	1406.5
1.4	10	2.9	1.6	152.7	87.3	8.4	1.2	65.0	1337.8
2.0	5	3.5	2.0	152.7	89.5	7.9	1.5	45.0	1943.8
Overall mean (<i>N</i> = 33)		2.7	1.5	121.0	67.3	11.8	1.9	50.0	
SD (<i>N</i> = 33)		1.3	0.7	106.8	66.6	6.4	1.6	46.2	
%CV (<i>N</i> = 33)		46.6	47.6	88.2	99.0	53.9	87.4	92.6	
Median (<i>N</i> = 33)		2.5	1.2	92.3	50.0	10.9	1.6	43.6	

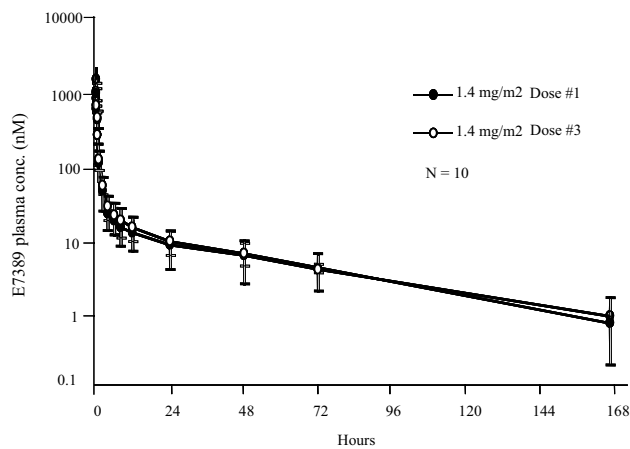


Fig. 1 Plasma concentration versus time profiles for E7389 for patients receiving 1.4 mg/m²

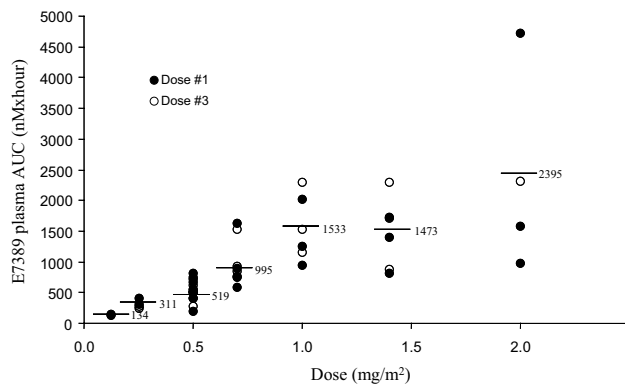


Fig. 2 E7389 AUC versus dose level

from each patient. Although none of the genes measured were significantly associated with response to E7389, there is preliminary evidence to suggest that lower intra-tumoral levels of β -tubulin III or higher intra-tumoral levels of MAP4 may correlate with response to E7389, while lower intra-tumoral levels of stathmin may be associated with progression (Fig. 4).

Discussion

The potent anticancer activity of halichondrin B, a natural product isolated from the *Halichondria okadai* black sea sponge [20], was discovered in 1986 [9]. Halichondrin B is a large polyether macrolide which exerts potent anticancer effects in cell-based and animal models of cancer [9–11]. The modified and synthetically produced analog, E7389 (eribulin mesylate, NSC 707389), is an analog of the biologically active macrocyclic portion of the natural product and shows similar anticancer properties in preclinical models [4].

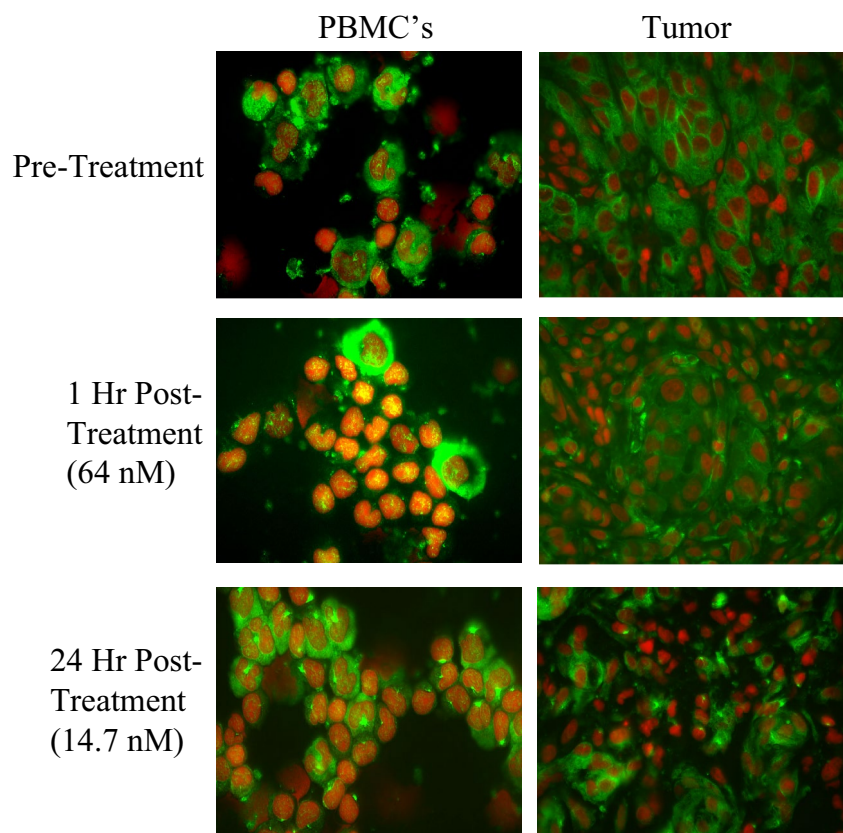
The initial 1986 report of halichondrin B activity in vivo demonstrated inhibition of tumor growth and increased host survival in the murine B16 melanoma and P388 and L1210 leukemia models at low exposure levels (2.5–100 μ g/kg) [9]. Subsequent studies by NCI investigators and others using human xenograft models documented increased survival rates, tumor growth delays, and reductions in size and number of metastases [12, 21]. Responses ranged from tumor growth inhibition to tumor regression to eradication of tumors. Testing of halichondrin B in the LOX and THS melanoma, OHS osteosarcoma, AHX, NCI-H522 and LXFS 538 lung cancer, KM 20L colon cancer, MDA-MB-435 breast cancer, and NIH:OVCAR-3 ovarian cancer xenograft models using several schedules and routes demonstrated that an intermittent iv regimen was associated with the greatest efficacy [12, 21].

In the MDA-MB-435 model, E7389 activity surpasses that of paclitaxel by 10- to 40-fold on a per dose basis and has a wide therapeutic window. 95 % tumor reductions were seen over a fourfold dosing range (0.25–1.0 mg/kg) with no evidence of toxicity based on body weight and water consumption. In comparison, the therapeutic window for paclitaxel in this model is 1.7, with complete tumor suppression seen only at its MTD of 25 mg/kg. Efficacy studies in the MDA-MB-435 breast, COLO 205 colon, and LOX melanoma models suggest a superior time to progression of E7389 compared with paclitaxel at its MTD following cessation of treatment [4].

Toxicology studies of E7389 given i.v. once daily on days 1, 5, and 9 produced bone marrow depression in dogs and rats, intestinal toxicity in dogs, and liver toxicity in rats. The MTD in rats was less than 0.25 mg/kg/day (1.5 mg/m²/day) given on days 1, 5, and 9. In dogs, E7389 was lethal at doses of 0.075 mg/kg/day (1.5 mg/m²/day) given as a 1-h infusion on days 1 and 5. Reversible myelosuppression occurred in dogs given 0.03 mg/kg/day (0.6 mg/m²/day) on days 1, 5, and 9. The clinical data noted in our study confirm the preclinical toxicity observations.

This trial employed a two-stage design utilizing an accelerated dosage escalation of intravenous halichondrin B analog (E7389, eribulin), followed by a more traditional schema following the observation of “moderate” toxicity. The accelerated portion of the dosage escalation was discontinued with the observation of one episode of reversible elevation of alkaline phosphatase. The eventual dose-limiting toxicity was noted to be reversible myelosuppression accompanied by fever. The MTD (1.4 mg/m²/week) determined by this current phase I study in humans is in concordance with the toxic dose on this schedule in preclinical and other phase I studies utilizing similar patient populations [22] and varying schedules of administration [23]. Response data suggest potential efficacy across a range of

Fig. 3 Microtubule morphologic changes in PBMCs and tumor from a patient receiving E7389. Peripheral blood mononuclear cells (PBMCs) and serial tumor biopsy specimens were collected from pt #12 (metastatic NSCLC) prior to dose 1 of cycle 1 and then again 1 and 24 h post-E7389 infusion. Cytospins were made from the PBMCs, and 0.2-micron slides were cut from the tumor blocks and de-paraffinized prior to labeling. Slides were dual labeled for beta-tubulin (*green*) and DNA (*red*) and imaged by laser scanning fluorescence microscopy. The plasma E7389 concentrations measured at the corresponding collection times of the PBMC and tumor specimens are indicated on the *left*



tumor types including NSCLC, breast and urothelial cancers, and melanoma.

Jordan et al. [5] have elucidated the unique mechanism of action of E7389 on microtubule dynamics. Like most other microtubule-targeted antitumor drugs, E7389 inhibits tumor cell proliferation in association with G₂-M arrest by binding to tubulin and inhibiting microtubule polymerization. However, unlike vinca alkaloids and taxanes that suppress both the shortening and growth phases of microtubule dynamics, E7389 seems to work by a novel end-poisoning mechanism, resulting predominantly in inhibition of microtubule growth, but not shortening. The effects of E7389 on microtubule dynamics appear to be concentration dependent, such that lower drug concentrations (~1 nM) alter the growth phase by directly binding to the growing microtubule ends, while at higher concentration E7389 induces the formation of tubulin aggregates, thereby reducing the amount of soluble tubulin available for microtubule elongation. Our own evaluation of cytoskeletal morphologic changes in PBMCs and tumor serves as an *in vivo* illustration of the dramatic effects of E7389 on microtubule structure (Fig. 3). These data confirm that E7389 is getting to the site of the tumor and affecting microtubule dynamics in a profound way.

Despite having unique mechanisms of microtubule disruption, alterations in the tubulin pathway have been

associated with resistance to taxanes [24–27], epothilones [26], and vinca alkaloids [28]. Alterations associated with resistance to these agents include tubulin isotype overexpression, β -tubulin mutations, and alterations in the levels of accessory proteins such as the microtubule-associated proteins MAP4, and stathmin [28]. In particular, considerable evidence exists to suggest that class III β -tubulin expression may be an important determinant of response to anti-microtubule agents. Increased β III-tubulin expression has been associated with resistance to taxanes and vincas in lung [29], breast [30], and ovarian cancers [31]. Therefore, we sought to evaluate potential relationships between tumoral gene expression and response to E7389. Although very preliminary, our results are consistent with those reported for other tubulin-targeted drugs, indicating that lower tumoral expression of β III-tubulin may be associated with a higher likelihood of response to E7389 treatment (Fig. 4). More data, from both the laboratory and the clinic, are needed before any conclusions can be drawn.

MAP4 is an accessory protein that binds to and stabilizes microtubules, and increased MAP4 expression leads to decreased sensitivity to microtubule-depolymerizing agents [28–32]. Stathmin is another microtubule-related protein that has been shown to regulate microtubule polymer mass, and increased expression has also been associated with resistance to anti-microtubule agents [32–34].

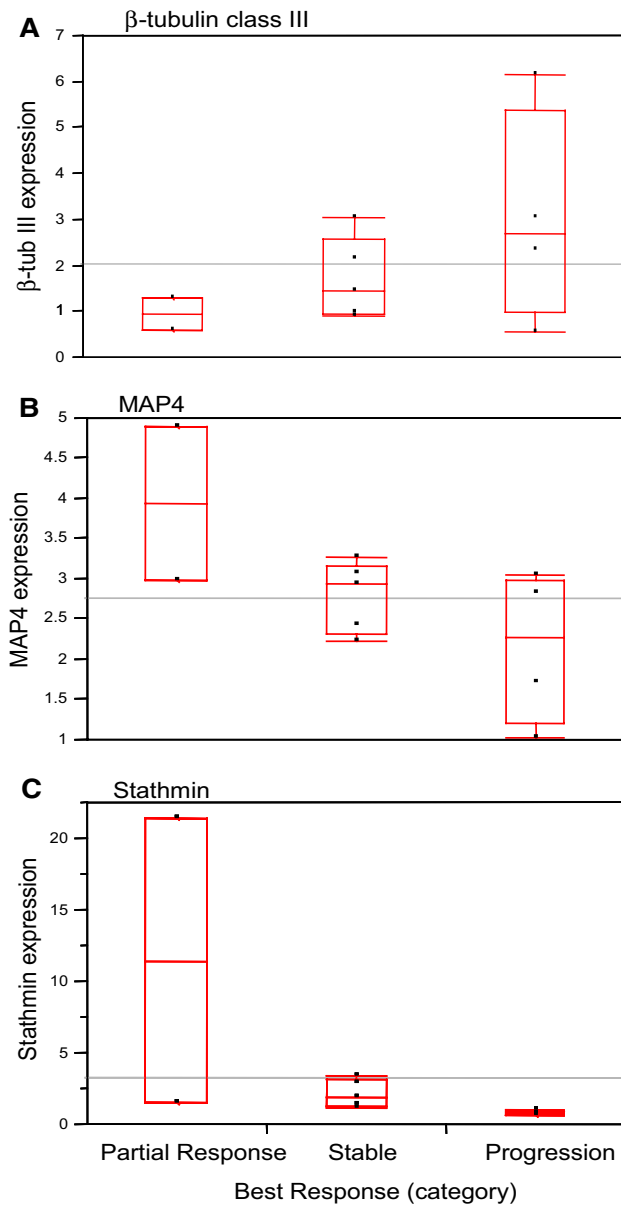


Fig. 4 Tumoral expression of β -tubulin III, MAP4, and stathmin versus response to 7389. Partial response ($n = 2$), stable disease ($n = 5$), progressive disease ($N = 4$)

The hypothesis generated from MAP4 and stathmin tumor expression data in the current study in association with response or progression on E7389 is actually the opposite of what has been reported for taxanes and vincas. While it is intriguing to speculate whether this might be related to differences in the mechanisms of action, as with β III-tubulin, these hypotheses require much more investigation.

Tubulin-targeted agents have become important agents used in the treatment of multiple solid tumors and are considered first-line therapy in lung, melanoma, and urothelial

tumors. The marked partial response data noted in this phase I study suggest that further evaluation of the activity of E7389 is warranted, either in combination or as a single agent in these and other tumors sensitive to this class of chemotherapeutic agents. The mild toxicity that we observed in this trial suggests that this agent is an excellent addition to the chemotherapeutic armamentarium. Additional clinical studies of E7389, alone and in combination, in lung, breast, and urothelial cancers have been performed and have confirmed that this agent is active and tolerable [35–37].

Acknowledgments This study was supported in part by National Cancer Institute Grants P30CA033572, UM1CA186717, U01CA062505, and M01RR000043.

References

- Margolin K, Synold T, Longmate J, Doroshow JH (2001) Methodologic guidelines for the design of high-dose chemotherapy regimens. *Biol Blood Marrow Transpl* 7(8):414–432
- Kraljevic S, Sedic M, Scott M, Gehrig P, Schlapbach R, Pavelic K (2006) Casting light on molecular events underlying anti-cancer drug treatment: what can be seen from the proteomics point of view? *Cancer Treat Rev* 32(8):619–629
- Collins I, Workman P (2006) New approaches to molecular cancer therapeutics. *Nat Chem Biol* 2(12):689–700
- Towle MJ, Salvato KA, Budrow J, Wels BF, Kuznetsov G, Aalfs KK, Welsh S, Zheng W, Seletsk BM, Palme MH, Habgood GJ, Singer LA, DiPietro LV, Wang Y, Chen JJ, Quincy DA, Davis A, Yoshimatsu K, Kishi Y, Yu MJ, Littlefield BA (2001) In vitro and in vivo anticancer activities of synthetic macrocyclic ketone analogues of halichondrin B. *Cancer Res* 61(3):1013–1021
- Jordan MA, Kamath K, Manna T, Okouneva T, Miller HP, Davis C, Littlefield BA, Wilson L (2005) The primary anti-mitotic mechanism of action of the synthetic halichondrin E7389 is suppression of microtubule growth. *Mol Cancer Ther* 4(7):1086–1095
- Perez EA (2009) Microtubule inhibitors: differentiating tubulin-inhibiting agents based on mechanisms of action, clinical activity, and resistance. *Mol Cancer Ther* 8(8):2086–2095
- Jimeno A (2009) Eribulin: rediscovering tubulin as an anticancer target. *Clin Cancer Res* 15(12):3903–3905
- Okouneva T, Azarenko O, Wilson L, Littlefield BA, Jordan MA (2008) Inhibition of centromere dynamics by eribulin (E7389) during mitotic metaphase. *Mol Cancer Ther* 7(7):2003–2011
- Hirata Y, Uemura D (1986) Halichondrins-antitumor polyether macrolides from murine sponges. *Pure Appl Chem* 58:701–710
- Bai R, Cichacz ZA, Herald CL, Pettit GR, Hamel E (1993) Spongistatin 1, a highly cytotoxic, sponge-derived, marine natural product that inhibits mitosis, microtubule assembly, and the binding of vinblastine to tubulin. *Mol Pharmacol* 44(4):757–766
- Bai RL, Paull KD, Herald CL, Malspeis L, Pettit GR, Hamel E (1991) Halichondrin B and homohalichondrin B, marine natural products binding in the vinca domain of tubulin. Discovery of tubulin-based mechanism of action by analysis of differential cytotoxicity data. *J Biol Chem* 266(24):15882–15889
- Fodstad O, Breistol K, Pettit GR, Shoemaker RH, Boyd MR (1996) Comparative antitumor activities of halichondrins and vinblastine against human tumor xenografts. *J Exp Ther Oncol* 1(2):119–125

13. Luduena RF, Roach MC, Prasad V, Pettit GR (1993) Interaction of halichondrin B and homohalichondrin B with bovine brain tubulin. *Biochem Pharmacol* 45(2):421–427
14. Hamel E (1992) Natural products which interact with tubulin in the vinca domain: maytansine, rhizoxin, phomopsis A, dolastatins 10 and 15 and halichondrin B. *Pharmacol Ther* 55(1):31–51
15. Smith JA, Wilson L, Azarenko O, Zhu X, Lewis BM, Littlefield BA, Jordan MA (2010) Eribulin binds at microtubule ends to a single site on tubulin to suppress dynamic instability. *Biochemistry* 49(6):1331–1337
16. Kuznetsov G, Towle MJ, Cheng H, Kawamura T, TenDyke K, Liu D, Kishi Y, Yu MJ, Littlefield BA (2004) Induction of morphological and biochemical apoptosis following prolonged mitotic blockage by halichondrin B macrocyclic ketone analog E7389. *Cancer Res* 64(16):5760–5766
17. Simon R, Freidlin B, Rubinstein L, Arbuck SG, Collins J, Christian MC (1997) Accelerated titration designs for phase I clinical trials in oncology. *J Natl Cancer Inst* 89(15):1138–1147
18. Towle MJ, Agoulnik S, Kuznetsov G, TenDyke K, Reardon C, Cheng H, Zheng W, Seletsky BM, Palme MH, Kishi Y, Lewis MD, Yu MJ, Littlefield BA (2003) In vivo efficacy of E7389, a synthetic analog of the marine sponge antitubulin agent halichondrin B, against human tumor xenografts under monotherapy and combination therapy conditions. *Proc Am Assoc Cancer Res* 44:628
19. McDaid HM, Mani S, Shen HJ, Muggia F, Sonnichsen D, Horwitz SB (2002) Validation of the pharmacodynamics of BMS-247550, an analogue of epothilone B, during a phase I clinical study. *Clin Cancer Res* 8(7):2035–2043
20. Simmons TL, Andrianasolo E, McPhail K, Flatt P, Gerwick WH (2005) Marine natural products as anticancer drugs. *Mol Cancer Ther* 4(2):333–342
21. Alley M, Dykes D, Waud W, Pacula-Cox D, Munro M, Newman D, Sausville E (1998) Efficacy evaluations of halichondrin B in selected xenografts. *Proc Am Assoc Cancer Res* 26:A1545
22. Goel S, Mita AC, Mita M, Rowinsky EK, Chu QS, Wong N, Desjardins C, Fang F, Jansen M, Shuster DE, Mani S, Takimoto CH (2009) A phase I study of eribulin mesylate (E7389), a mechanistically novel inhibitor of microtubule dynamics, in patients with advanced solid malignancies. *Clin Cancer Res* 15(12):4207–4212
23. Tan AR, Rubin EH, Walton DC, Shuster DE, Wong YN, Fang F, Ashworth S, Rosen LS (2009) Phase I study of eribulin mesylate administered once every 21 days in patients with advanced solid tumors. *Clin Cancer Res* 15(12):4213–4219
24. Giannakakou P, Poy G, Zhan Z, Knutsen T, Blagosklonny MV, Fojo T (2000) Paclitaxel selects for mutant or pseudo-null p53 in drug resistance associated with tubulin mutations in human cancer. *Oncogene* 19(27):3078–3085
25. Day BW (2000) Mutants yield a pharmacophore model for the tubulin–paclitaxel binding site. *Trends Pharmacol Sci* 21(9):321–324
26. Giannakakou P, Gussio R, Nogales E, Downing KH, Zaharevitz D, Bollbuck B, Poy G, Sackett D, Nicolaou KC, Fojo T (2000) A common pharmacophore for epothilone and taxanes: molecular basis for drug resistance conferred by tubulin mutations in human cancer cells. *Proc Natl Acad Sci USA* 97(6):2904–2909
27. Monzo M, Rosell R, Sanchez JJ, Lee JS, O’Brate A, Gonzalez-Larriba JL, Alberola V, Lorenzo JC, Nunez L, Ro JY, Martin C (1999) Paclitaxel resistance in non-small-cell lung cancer associated with beta-tubulin gene mutations. *J Clin Oncol* 17(6):1786–1793
28. Kavallaris M, Tait AS, Walsh BJ, He L, Horwitz SB, Norris MD, Haber M (2001) Multiple microtubule alterations are associated with Vinca alkaloid resistance in human leukemia cells. *Cancer Res* 61(15):5803–5809
29. Gan PP, Pasquier E, Kavallaris M (2007) Class III {beta}-tubulin mediates sensitivity to chemotherapeutic drugs in non small cell lung cancer. *Cancer Res* 67(19):9356–9363
30. Tommasi S, Mangia A, Lacalamita R, Bellizzi A, Fedele V, Chiriatti A, Thomssen C, Kendzierski N, Latorre A, Lorusso V, Schittulli F, Zito F, Kavallaris M, Paradiso A (2007) Cytoskeleton and paclitaxel sensitivity in breast cancer: the role of beta-tubulins. *Int J Cancer* 120(10):2078–2085
31. Mozzetti S, Ferlini C, Concolino P, Filippetti F, Raspaglio G, Prislei S, Gallo D, Martinelli E, Ranelletti FO, Ferrandina G, Scambia G (2005) Class III beta-tubulin overexpression is a prominent mechanism of paclitaxel resistance in ovarian cancer patients. *Clin Cancer Res* 11(1):298–305
32. Martello LA, Verdier-Pinard P, Shen HJ, He L, Torres K, Orr GA, Horwitz SB (2003) Elevated levels of microtubule destabilizing factors in a Taxol-resistant/dependent A549 cell line with an alpha-tubulin mutation. *Cancer Res* 63(6):1207–1213
33. Alli E, Bash-Babula J, Yang JM, Hait WN (2002) Effect of stathmin on the sensitivity to antimicrotubule drugs in human breast cancer. *Cancer Res* 62(23):6864–6869
34. Burkhardt CA, Kavallaris M, Band HS (2001) The role of beta-tubulin isotypes in resistance to antimitotic drugs. *Biochim Biophys Acta* 1471(2):O1–O9
35. Cortes J, O’Shaughnessy J, Loesch D, Blum JL, Vahdat LT, Petrakova K, Chollet P, Manikas A, Dieras V, Delozier T, Vladimirov V, Cardoso F, Koh H, Bougnoux P, Dutcus CE, Seegobin S, Mir D, Meneses N, Wanders J, Twelves C (2011) Eribulin monotherapy versus treatment of physician’s choice in patients with metastatic breast cancer (EMBRACE): a phase 3 open-label randomised study. *Lancet* 377(9769):914–923
36. Scarpace SL (2012) Eribulin mesylate (E7389): review of efficacy and tolerability in breast, pancreatic, head and neck, and non-small cell lung cancer. *Clin Ther* 34(7):1467–1473
37. Gitlitz BJ, Tsao-Wei DD, Groshen S, Davies A, Koczywas M, Belani CP, Argiris A, Ramalingam S, Vokes EE, Edelman M, Hoffman P, Ballas MS, Liu SV, Gandara DR (2012) A phase II study of halichondrin B analog eribulin mesylate (E7389) in patients with advanced non-small cell lung cancer previously treated with a taxane: a California Cancer Consortium trial. *J Thorac Oncol* 7(3):574–578